Plasmonics (2023) 18:1075–1081
https://doi.org/10.1007/s11468-023-01835-8

RESEARCH

Green Synthesis of Silver Nanoparticles Using *Argyreia nervosa* Leaf Extract and Their Antimicrobial Activity

K. Parvathalu[1] · S. Chinmayee[1] · B. Preethi[1] · A. Swetha[1] · G. Maruthi[1] · M. Pritam[5] · B. Sreenivas[4] · S. Ramu Naidu[2] · G.L. Merlinsheeba[3] · B. Murali[2] · M. Vijay[3] · K. Moses[6] · D. Chinni Krishna[1] · P. Bala Bhaskar[1]

Received: 8 March 2023 / Accepted: 29 March 2023 / Published online: 6 April 2023

Abstract

The biogenic synthesis of silver nanoparticles (AgNPs) has attracted many researchers due to their physical, chemical, optical, and biological properties, embracing a range of activities such as antibacterial, antifungal, anti-inflammatory, and anticancer activities. The purpose of this work is to synthesize and characterize AgNPs using *Argyreia nervosa* (AN) plant leaf extract, as well as to test their antimicrobial applications. In this work, silver nitrate ($AgNO_3$) at 0.1 mM concentration and stable AgNPs were synthesized and observed by monitoring the color change of the solution from light yellow to brown. The UV–Vis spectrum shows a peak at 445 nm, confirming the formation of AN-AgNPs and Fourier transform infrared (FTIR) results confirm the presence of chemical groups which act as reducing agents stabilizing the AN-AgNPs and antimicrobial capping agents enhancing antimicrobial properties of AN-AgNPs. The crystalline behavior of these AN-AgNPs is confirmed through X-ray powder diffraction (PXRD) peaks. The morphology of AN-AgNPs and their sizes were studied (sizes range from 10 to 40 nm) using scanning electron microscopy (SEM). The disk diffusion assay shows the antimicrobial activity over *Escherichia coli* pathogenic microorganisms of clinical interest. The obtained results confirm a more significant antimicrobial effect of the biogenic AN-AgNPs maintaining low cytotoxicity. This work presents a potential way to produce non-toxic biogenic AgNPs with enhanced antibacterial activity, which can meet the increasing global demand for biogenic AgNPs as an alternative to antibiotics.

Keywords Silver nanoparticles · Green synthesis · Crystalline · Antibacterial activity

Introduction

The nano-material research encourages designing different types of nano-scale devices. Nanoparticles (NPs) with a size range of 1–100 nm and different shapes provide unique physical, chemical, optical, and biological properties [1–3]. Nanotechnology is the most used research field in translational research that integrates all disciplines of engineering and sciences. Nanotechnology has created many opportunities in all material industries such as electronics, biotechnology, healthcare, agriculture, and tissue engineering [4–6]. Metal nanoparticles have gained attention for biomedical applications due to their multifunctional properties. Extensive research has been done on silver nanoparticles (AgNPs) owing to their broad range of industrial applications such as water purification, antimicrobial, medical devices, sensors, and the food industry [7–12]. The chemical and physical methods are used in the synthesis of metal nanoparticles, but they are capped or stabilized with hazardous chemicals [13]. Alternatively, green synthesis is the best method because of the low

✉ K. Parvathalu
parvathalu.k@gmail.com

1 Department of Physics, Government City College (A), Nayapul, Osmania University, 500002 Hyderabad, Telangana, India

2 Department of Chemistry, University of Hyderabad, 500046 Hyderabad, Telangana, India

3 Department of Biochemistry, University of Hyderabad, 500046 Hyderabad, Telangana, India

4 Department of Chemistry and Biosciences, Rice University-BRC, 77005 Houston, TX, USA

5 Department of Physics, Michigan Technological University, 49931 Houghton, MI, USA

6 Department of Chemistry, Faculty of Science and Education, Busitema University, Tororo, Uganda

toxicity, low cost, eco-friendly, and easy processing [14–16]. Furthermore, plants, leaves, and fruits are easily available resources of bioactive phytochemicals such as proteins, polyphenols, flavonoids, alkaloids, amines, ketones, and aldehydes, which act as reducing, stabilizing, and capping agents in the process of conversion of metal ions to metal nanoparticles, leading to the high production of metal nanoparticles with multifunctional properties. Among various metal nanoparticles, AgNPs have been placed as the top priority for the last two decades due to their unique applications in material, medical, and biomedical industries such as antimicrobial, anticancer, and photo-catalytic activity [17].

Plant-mediated and microorganisms are two primary sources to synthesize metal nanoparticles. Most plants have been found medically important to cure different diseases. Synthesized metal nanoparticles using plant leaf/root/fruit extracts are more advantageous than the synthesis of metal nanoparticles using microorganisms, since it does require complex processes such as isolation, culture maintenance, and many purification steps. With this, it has become a major focus for researchers to develop the green synthesis of metal nanoparticles using different parts of plants (leaf, peel, fruit, root, and flowers) [18–24]. The phytochemicals present in the plant extract play an important role in the process of conversion of metal ions into stable metal nanoparticles with potential applications [25–34].

Recent studies have been focused on the green synthesis of AgNPs using different plant leaves, but the biogenic of AgNPs using indigenous plant extracts exhibiting potential antibacterial and anticancer activity has not been studied to a large extent. *Argyreia* plant (AN) shows medicinal values such as antioxidant, antiulcer, antimicrobial, and antiviral. AN plant leaves have been used to treat diseases of the nervous system. With this knowledge of AN plant leaves, the synthesized silver nanoparticles using AN plant leaf extract help to study a potential effect of antimicrobial activity.

In this work, AgNPs were synthesized using AN leaf extract, where various phytochemical compounds present in AN were involved in the reduction of metal ions into metal nanoparticles (MNP) [35–45] The synthesized (AN-AgNPs) silver nanoparticles were characterized by using ultraviolet (UV)-Vis spectrometry, Fourier transform infrared (FTIR), X-ray powder diffraction (PXRD), scanning electron microscopy (SEM), and zeta potential. The antibacterial activity of the AN-AgNP was studied using the disk diffusion method.

Materials and Methods

Materials

Argyreia nervosa leaves were obtained from an herbal garden in the Hyderabad, India. All other chemicals such as silver nitrate and acetone were purchased from Sigma Aldrich, Bangalore, India.

Methodology

Argyreia nervosa (AN) leaves were cleaned and dried for a few days in normal sunlight. Then, AN leaves were grounded to make powder and 1 g of AN powder was added to 100 ml water. The mixture was heated for 30 min at 60 °C temperature under magnetic stirring of 500 rpm. Two hundred milliliters of silver nitrate solution with concentration 0.1 mM was prepared under magnetic stirring of 500 rpm at a temperature 80 °C. Then, AN extract solution was filled in the burette and added drop wise to 200 ml silver nitrate solution at 80 °C under 500 rpm magnetic stirring. The AN-AgNPs samples were collected with different concentrations. Finally, AN-AgNPs were separated by centrifugation (5000 rpm) and allowed to dry at 50 °C for further characterization process. The synthesis process is shown in Fig. 1.

Characterization of AN-AgNPs

UV Spectroscopy

The UV–Vis was used to see the formation of AN-AgNPs particles. The AN-AgNPs solution was scanned over the range of 250–800 nm by using a UVJASCO V-750 spectrometer.

Fourier Transform Infrared (FTIR) Spectroscopy

The IR spectra of AN leaf aqueous extract and the centrifuged AN-AgNPs sample were used to identify the possible phytochemical and biomolecules constituents involved in the synthesis and capping of AN-AgNPs. The samples were

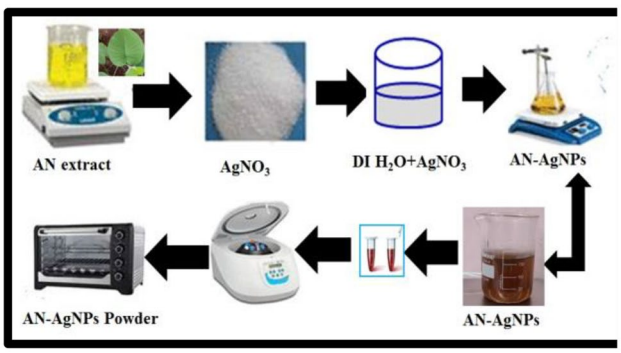

Fig. 1 Green synthesis process of AN-AgNPs

analyzed by IR Thermo Fisher Nicolet iS5. The spectra were recorded from 400 to 4000 cm^{-1}.

Scanning Electron Microscopy (SEM)

FE-SEM was used to characterize the morphology and particle size of AN-AgNPs. A thin film of oven-dried AN-AgNPs sample was prepared and used over a carbon-coated copper grid via a ZEISS Merlin Compact instrument operated at an accelerated voltage of 20 kV.

Zeta Potential and Zeta Seizer

The zeta potential of particles was analyzed by using the Zeta-sizer Nano-ZS. Measurements were carried out at 25 °C temperature in an aqueous media. The zeta potential was calculated from the electrophoretic (charge) mobility based on the Smoluchowski theory.

X-ray Powder Diffraction

The structure of nanoparticles was analyzed by using the XRD Bruker D8 Advance. The Miller indices and *d*-spacing were calculated from the PXRD data and data matching was done using X pert high Score software and then structure details were analyzed.

Antibacterial Activity of AN-AgNPs on EPEC by Evaluating the Disk Diffusion Method (DDM)

To detect the antibacterial potential of green synthesized AN-AgNPs against enteropathogenic *Escherichia coli* (EPEC), gentamycin is recommended to be used as one of the positive controls to test antimicrobial effect and Luria–Bertani broth (LB broth) is used as the negative control. EPEC (100 µl of OD 600 = 1) is plated on LB agar plates and disks coated with 50 µl of AN-AgNPs are placed and incubated for 12 h along with AN leaf extract control at 37 °C. The zone of inhibition is measured by calculating the diameter of the clear zone in cm.

Results and Discussions

The phytochemicals and biomolecules present in the extract could help to form active sites on the capping of metal nanoparticles. These flavonoids can donate an electron, and phenolics exhibit a chelating effect (a chemical compound that can bind tightly to metal ions) on the metal ions, which could be responsible for reducing metal ions into metal nanoparticles. The characteristics of metal nanoparticles were studied using UV–Vis, FTIR, SEM, EDX, PXRD, and antibacterial activity [37].

Fourier Transform Infrared (FTIR) Spectroscopy

The FTIR spectra of the AN aqueous extract and AN-AgNPs were recorded to identify the probable biomolecules and phytochemical functional groups which could be responsible for the reduction and stability of AgNPs. The phytochemical profile of AN extract aqueous shows transmission peaks at 496, 595, 1300, 1670, 2363, and 3308 cm^{-1}, respectively (Fig. 2). The phytochemical profile of AN-AgNPs shows suppression of all transmission peaks except at 1670 and 3308 cm^{-1}. The FTIR band at 3308 cm^{-1} is assigned to the intermolecular H bands, most probably water molecules and 1670 cm^{-1} is attributed to N–H stretching in amines, and C = 0 stretching of ketones or acids. All the vibrational peaks in the AN extract spectrum were suppressed, and we observed more transmission peaks. The phenolic structure in plant leaf extract plays a vital role in reducing and stabilizing metal ions into metal nanoparticles. The abundance of the alcohol group makes it a powerful antioxidant and a strong reducing agent for the formation of metal nanoparticles. Furthermore, the biomolecules in the plant leaf extract play a dual role of reducing and capping of formation of AgNPs.

UV–Vis Absorption Spectroscopy

The formation of AgNPs was first identified by a visual color change in $AgNO_3$ and with a control drop rate of AN extract in $AgNO_3$ solution, as time increased. The color of the mixture gradually changes from yellowish to brown confirming the formation of AN-AgNPs. This might be due to the reduction of the silver ions leading to the excitation of surface plasmon resonance (SPR) of the AN-AgNPs. To confirm this, the UV–Vis absorption spectra (wavelength range: 200–700 nm) was recorded from each synthesized set of AN-AgNPs at different concentrations.

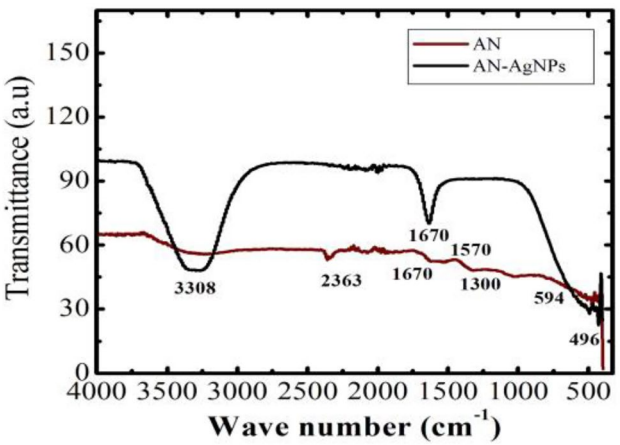

Fig. 2 FTIR spectrum of AN and AN-AgNPs

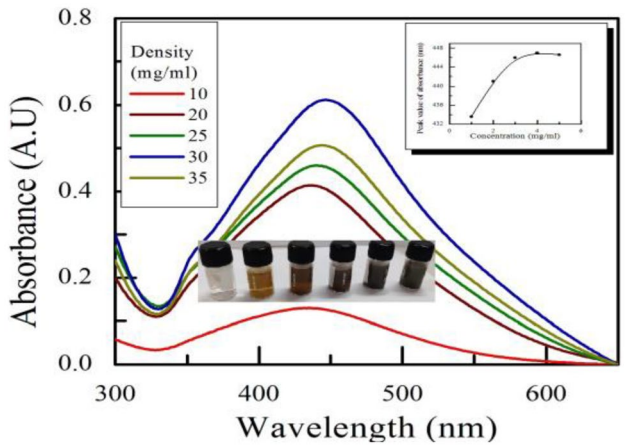

Fig. 3 UV spectrum of AN-AgNPs

Biogenic AN-AgNPs show the maximum absorbance at 445 nm which shows stable range for AgNPs formation. The AN-AgNPs colloidal solution shows distinct peaks from 442 to 450 nm for different AgNP concentrations. The UV–Vis scan of the sodium-citrated stabilized AgNPs colloidal solution shows peak at 430 nm [35]. The AN-AgNPs colloidal solution observed distinct peaks from 470 to 490 nm for different AgNPs concentrations. It was observed that AN stabilized AgNPs colloidal solution absorption peak shifted from shorter wavelengths to longer wavelengths, and it might be due to the size variation of metal nanoparticles leading to change of specific surface area (inserted in Fig. 3).

Scanning Electron Microscopy

The morphological study of biogenic AN-AgNPs was investigated by field emission scanning electron microscopy (FE-SEM). Figure 4 shows the presence of spherical shape metal nanoparticles with different sizes ranging from 30 to 40 nm. The average particle size was measured to be approximately 20 nm. The particle size distribution was calculated from a histogram, considering 200 particles, from which, the average AN-AgNPs size was measured using the Image-J software. The metal nanoparticles were well dispersed and not in direct contact with each other, which could be explained by the stabilizing action of capping agents present in the AN

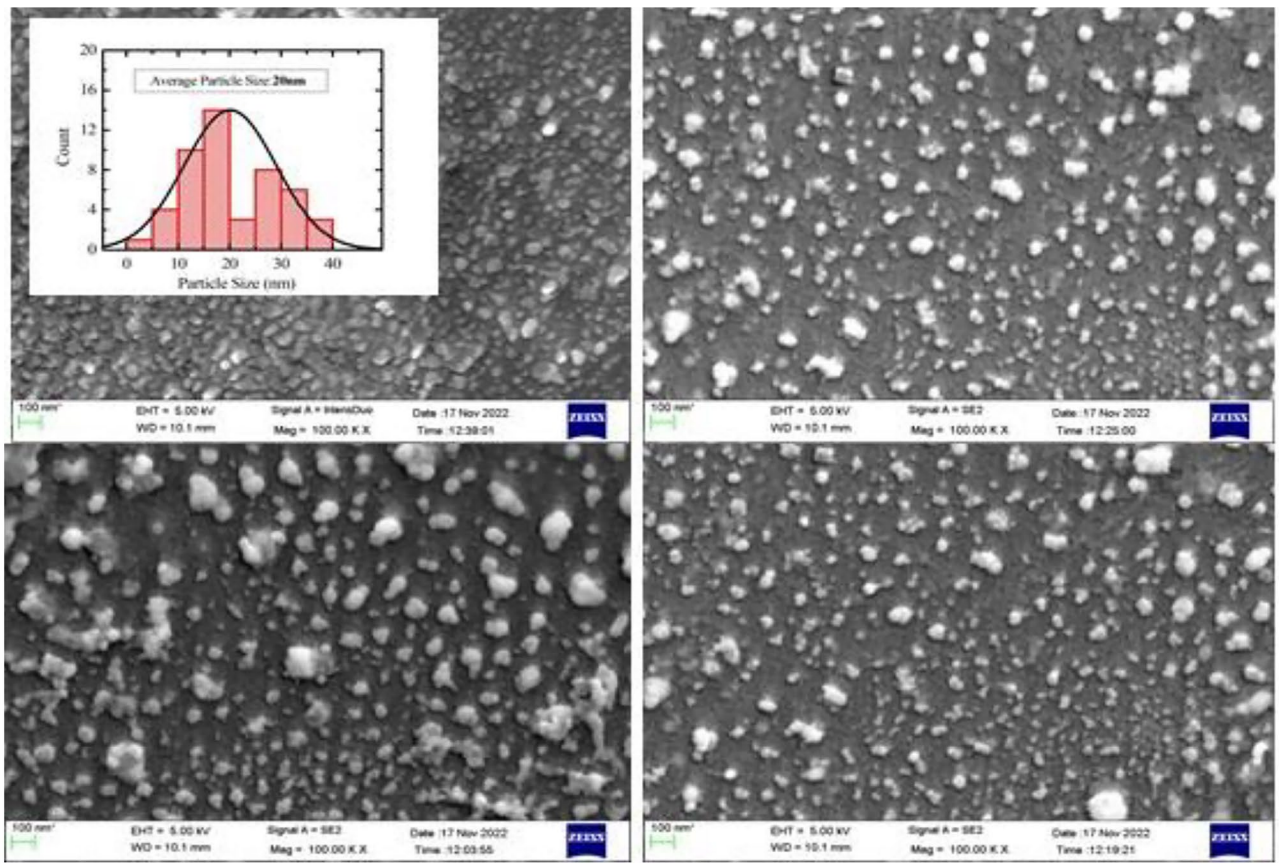

Fig. 4 SEM images of AN-AgNPs

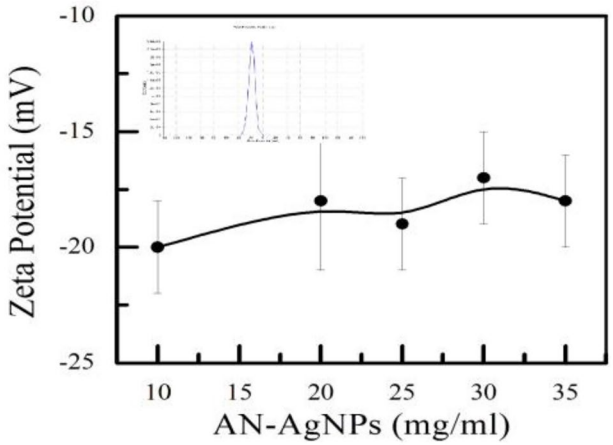

Fig. 5 Zeta potential as a function of GT-AgNPs

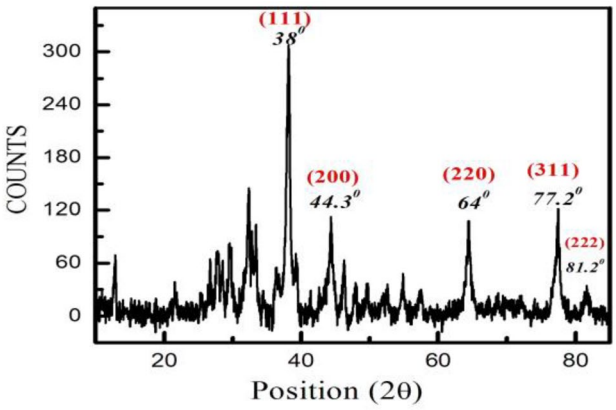

Fig. 6 PXRD pattern of AN-AgNPs: face-centered cubic (FCC) crystal structure of silver

extract. This clearly shows that particles are dispersed in a homogeneous manner and play an important role in different biomedical activities. The FE-SEM confirms that the metal nanoparticles were dispersed in uniform distribution with spherical shapes of the silver nanoparticles.

Zeta Potential and Zeta Seizer

The change of zeta potential as a function of AN-AgNPs concentration is shown in Fig. 5. The surface potential of metal nanoparticles is the potential difference between the medium where the metal nanoparticles are dispersed and the accessible surface of dispersed metal nanoparticles which can be analyzed using zeta seizer. This property plays an important role to understand the surface interaction of metal nanoparticles and indicating the long-term stability of the dispersion. The zeta potential of AN-AgNPs shows stability as the function of AN-AgNPs concentration. Figure 5 shows that zeta potential value of biosynthesized AN-AgNPs was found to be −21 mV. For synthesized nanoparticles, the values of zeta potential greater than + 25 mV or less than −25 mV have high degrees of stability. It indicates that the AN-AgNP particles show highly stable in colloidal solution.

X-ray Powder Diffraction (PXRD) Analysis

The crystalline nature of biogenic AN-AgNP nanoparticles was confirmed by X-ray diffraction pattern. The phase matching was done through X-pert high score plus software and data were collected through the PXRD instrument, with Cu Kα radiation ($\lambda = 0.1541$ nm) over the processing range $2\theta = 10$–$90°$, with a step of 0.02°. The PXRD pattern of biosynthesized AN-AgNPs (Fig. 6) shows several peaks, where the four main peaks are located at 38°, 44.3°, 64°, and 77.2°, corresponding to the (111), (200), (220), and (311) reflection planes, respectively, to the structure of face-centered cubic (FCC) crystal of silver (JCPDS, No. 04–0783) [46]. In addition to Braggs peaks for silver nano-crystal, additional peaks were observed at 16.9°, 29.6°, and 33.6°. The presence of these additional peaks might be due to AN extract which contains biomolecules suggesting that the crystallization of bio-organic phase occurs on the surface of AgNPs. On the basis of Bragg's diffraction angle (2θ) and the full width of half maximum (β) for more intense peaks (111), corresponding average crystalline size was calculated as 22 nm. The average size of the crystalline was calculated based on the Debye–Scherrer equation. The details of lattice parameters, cell volume, and crystalline size are mentioned in Table 1.

The size of the crystalline AN-AgNPs was calculated using the Debye–Scherrer formula.

$$Crystalline\ size\ (D) = \frac{0.9\lambda}{\beta Cos\theta} \quad (1)$$

where λ is the X-ray wavelength (0.1541 nm), β is the full width of half maximum (FWHM) (line broadening at half maximum) in radians, and 2θ is the Bragg's angle. Crystalline size for all planes is mentioned in Table 1.

Antibacterial Activity

The antimicrobial activity of the aqueous AN plant's leaf extract and biogenic AN-AgNPs was carried out by the disk diffusion method against pathogenic organism *E. coli*, Luria–Bertani broth (negative control) [47–49], and gentamycin (positive control) as shown in Fig. 7. AN-AgNPs showed higher antibacterial activity in terms of zone of inhibition against *E. coli* when compared to the aqueous leaf extract of AN. The zone of inhibition was observed 11 mm for all concentration of

Table 1 Crystalline parameters for different planes

S.NO	Planes (hkl)	2θ	FWHM (β) radians	Interplanar spacing (d)	Lattice constant (a)	Cell volume (a^3)	Crystalline size (D) nm $k\lambda/\beta Cos\theta$; k–0.9; λ–0.1541
1	111	38	0.0066	2.2	4.1	64	22
2	200	44	0.0041	2.1	4.2	74	36
3	220	64	0.0075	1.5	4.2	74	22
4	311	77	0.0058	1.3	4.3	79	31

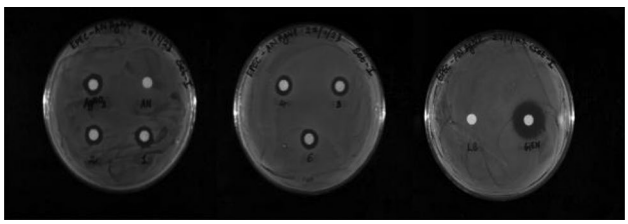

Fig. 7 Antimicrobial susceptibility conducted through disk diffusion method. Zones of inhibition of different concentrations of biogenic AN-AgNPs showed against *E. coli*, AN extract, LB broth (negative control), and gentamicin (positive control)

AN-AgNPs within the error bars against *E. coli* and this concentration of AN-AgNP is efficient enough to remove bacteria colony. The aqueous leaf extract did not show antibacterial activity. The zone of inhibition on bacterial strain was measured after 12 h of incubation at 37 °C. The zone of inhibition on bacterial strain is shown in Fig. 8 as a function AN-AgNPs concentration.

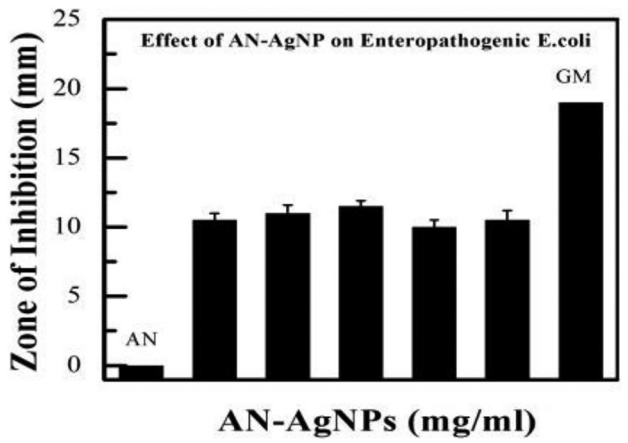

Fig. 8 Zones of inhibition is the function of concentrations of biogenic AN-AgNPs against *E. coli*

Conclusions

In this work, the green synthesis of silver nanoparticles from *Argyreia nervosa* (AN) plant's leaf extract was observed under UV–Vis spectroscopy at 445 nm and the biomolecules involved in the reduction of Ag^+ ions to Ag nanoparticles were identified using FTIR spectroscopy. The crystalline nature of silver nanoparticles was confirmed using XRD study. AgNPs are found to be very effective to act as an antibacterial agent. As these nanoparticles are non-toxic and safe in vivo studies, the green synthesized silver nanoparticles can be used for the treatment of different diseases. The antibacterial activity of prepared AN-AgNPs was evaluated using disk diffusion assay and these AN-AgNPs showed potential antibacterial activity against the enteropathogenic *E. coli* bacteria strain. Our findings open one potential path to produce biogenic AgNPs, to meet the increasing global demand for their applications as an alternative to antibiotics. However, there must be more experiments be carried out to find the evaluation of efficacy on animals as well as human beings and further research on AN-AgNPs is needed to explore potential applications in bio-nano-medical technology.

Acknowledgements The authors would like to thank to Department of Chemistry, Department of Biochemistry, University of Hyderabad, Hyderabad, Government City College (A), Osmania University, Hyderabad, Telangana, for providing facilities.

Author Contribution K. Parvathalu, S. Chinmayee, B. Preethi, A. Swetha, S. Ramu Naidu, and Merlinsheeba have been contributed data collection. K. Parvathalu analyzed data and drafted manuscript. M. Pritam, B. Sreenivas, B. Murali, M. Vijay, K. Moses, D. Chinni Krishna, and P. Bala Bhaskar helped in discussion part of the project at various levels.

Funding The authors would like to thank to Commissionerate of Collegiate Education (CCE), Telangana, India, for providing funding support.

Data Availability The authors are going to provide data of any specific analysis.

Declarations

Conflict of Interest The authors declare no competing interests.

References

1. Shenton W, Douglas T, Young M, Stubbs G, Mann S (1999) Adv Mater 11:23–256
2. Tang S, Mao C, Liu Y, Kelly DQ, Banerjee SK (2007) IEEE Trans
3. Thakkar K, Mhatre S, Parikh R (2009) Nanotechnol. Biol Med 6:257–262
4. Fakhari S, Jamzad M, Kabiri Fard H (2019) Green Chem Lett Rev 12:19–2
5. Ramsden J (2016) Nanotechnology:William Andrew
6. Ahmed S, Ahmad M, Swami B, Ikram S (2016) J Adv Res 7:17–28
7. Tang S, Mao C, Liu Y, Kelly DQ, Banerjee SK (2007) IEEE Trans
8. Thakkar K, Mhatre S, Parikh R (2009) Nanotechnol. Biol Med 6:257–262
9. Chen H, Roco MC, Li X, Lin Y (2008) Trends in nanotechnology patents. Nat Nanotechnol 3:123–125
10. Chen H, Roco MC, Li X, Lin Y (2008) Trends in nanotechnology patents. Nat Nanotechnol 3:123–125
11. Smetana AB, Klabunde KJ, Sorensen CM J (2005) Colloid Interface Sci 284:521–526
12. Lee H, Chou KS, Huang KC (2005) Nanotechnology 16:2436–2441
13. Shenton W, Douglas T, Young M, Stubbs G, Mann S (1999) Adv Mater 11:23–256
14. Wakuda D, Kim KS, Suganuma K (2008) Scripta Mater 59:649–652
15. Anna Z, Eva S, Adriana Z, Maria G, Jan H (2009) Procedia Chem 1:1560–1566
16. Kholoud MM, Abou E, Ala A, Abdulrhman Reda AAA (2010) Arab J Chem 3:135–140
17. Haggag EG, Elshamy AM, Rabeh MA, Gabr NM, Salem M, Youssif KA, Samir A, Bin Muhsinah A, Alsayari A, Abdelmohsen U (2019) R. Int J Nanomed 14:6217–6229
18. Iravani S (2011) Green Chem 13:2638–2650
19. Duan H, Wang D, Li Y (2015) Chem Soc Rev 44:5778–5792
20. Kumar V, Anthony S (2016) Surf Chem Nanobiomater 265–300
21. Hasan S (2015) Res J Recent Sci 4:1–3
22. Prabu HJ, Johnson I, Karbala (2015) Int J Mod Sci 1:237–246
23. Shakeel AH, Saifullah, MA, Babulal S, Saiqa I (2016) J Radiat Res Appl Sci 9:1–7
24. Khatoon A, Khan F, Ahmad N, Shaikh S, Rizvi SM, Shakil S, Al-Qahtani MH, Abuzenadah AM, Tabrez S, Ahmed AB, Alafnan A (2018) Life Sci 15:430–434
25. Annu S (2018) A, Gurpreet, K, Praveen, S, Sandeep, S, Saiqa, I. J Appl Biomed 16:221–231
26. Padalia H, Moteriya P, Chanda S (2015) Arab J Chem 8:732–741
27. Lakshmanan G, Sathiyaseelan A, Kalaichelvan PT, Murugesan K (2018) Karbala Int J Mod Sci 4:61–68
28. Benakashani F, Allafchian A, Jalali SAH (2017) Green Chem Lett Rev 10:324–330
29. Kumar DA, Palanichamyand V, Roopan SM (2014) Spectrochim Acta Part A 127:168 –171
30. Sankar R, Manikandan P, Malarvizhi V, Fathima T, Shivashangariand KS, Ravikumar V (2014) Spectrochim Acta Part A 121:746–750
31. Dhand V, Soumya L, Bharadwaj S, Chakra S, Bhattand D, Sreedhar B (2016) Mater Sci Eng C 58:36–43
32. Saifullah AS, Ahmad M, Swamiand BL, Ikram S, Radiat J (2016) Res Appl Sci 9:1–7
33. Khalil MM, Ismail EH, El-Baghdadyand KZ, Mohamed D (2014) Arabian J Chem 7:1131–1139
34. Ameen F, AlYahya S, Govarthanan M, ALjahdali N, Al-Enazi N, Alsamhary K, Alshehri WA, Alwakeeland SS, Alharbi SA (2020) J Mol Struct 1202:1272
35. Kalakonda P (2016) Nanomater Nanotechnol 6:1847980416663672
36. Kalakonda P, Banne S (2017) Plasmonics 12(4):1221
37. Kalakonda P, Banne S (2018) Plasmonics 13(4):1265
38. Parveen K, Banse V, Ledwani L (2016) AIP Conf Proc 1724:020048
39. Nune SK, Chanda N, Shukla R, Katti K, Kulkarni RR, Thilakavathyand S, Katti KV (2009) J Mater Chem 19:2912–2920
40. Widatalla HA, Yassin LF, Alrasheid AA, Ahmed SAR, Widdatallah MO, Eltilib SH, Mohamed AA (2022) 4(3):911–915
41. Sriramprabha R, Divagar M, Ponpandian N, Viswanathan C (2018) J Electrochem Soc 165:498-B507
42. Tangand S, Zheng J (2018) Adv Healthcare Mater 7:1701503
43. Le Ouayand B, Stellacci F (2015) Nano Today 10:339–354
44. Keshari AK, Srivastava R, Singh P, Yadavand VB, Nath G (2020) J Ayurveda Integr Med 11:37–44
45. Gandhiand H, Khan S (2016) J Nanomed Nanotechnol 7:1000366
46. Mani M, Harikrishnan R, Purushothaman P, Pavithra S, Rajkumar P, Kumaresan S, Dunia A, Al Farraj, Mohamed SE, Balamuralikrishnan B, Kaviyarasu S (2021) Environ Res 202:111627
47. Helen R, Jon G, Zachary H, Erin O (2021) Semmens, Elizabeth Williams, Erin L (2021) Landguth Environ Res 198:111195
48. Barbhuiya RI, Singha P, Asaithambi N, Singh SK (2022) Food Chem 385:132602
49. Mani M, Pavithra S, Mohanraj K, Kumaresan S, Saqer SA, Mostafa M, Eraqi A, Dhanesh G, Ranganathan B, Maaza M, Kaviyarasu K (2021) Environ Res 199:111274